NASA Technical Memorandum 100928
ICOMP–88–12

Improved Finite Strip Mindlin Plate Bending Element Using Assumed Shear Strain Distributions

Abhisak Chulya
Institute for Computational Mechanics in Propulsion
Lewis Research Center
Cleveland, Ohio

and

Robert L. Thompson
Lewis Research Center
Cleveland, Ohio

July 1988

NASA

IMPROVED FINITE STRIP MINDLIN PLATE BENDING ELEMENT

USING ASSUMED SHEAR STRAIN DISTRIBUTIONS

Abhisak Chulya*
Institute for Computational Mechanics in Propulsion
Lewis Research Center
Cleveland, Ohio 44135

and

Robert L. Thompson
National Aeronautics and Space Administration
Lewis Research Center
Cleveland, Ohio 44135

SUMMARY

A linear finite strip plate element based on Mindlin/Reissner plate theory is developed. The analysis is suitable for both thin and thick plates. In the formulation new transverse shear strains are introduced and assumed constant in each two-node linear strip. The element stiffness matrix is explicitly formulated for efficient computation and computer implementation. Numerical results showing the efficiency and predictive capability of the element for the analysis of plates are presented for different support and loading conditions and a wide range of thicknesses. No sign of shear locking phenomenon was observed with the newly developed element.

1. INTRODUCTION

The finite strip method, a combination of finite element and Fourier-series expansion, has important advantages for the analysis of a wide range of plate problems. The first finite strip bending element was developed following classical Kirchhoff thin plate theory (refs. 1 and 2). This formulation is very reliable for thin plate analysis but lack the ability to account for shear deformation which can be important when a plate becomes thick. In addition, displacement based finite element implementation of Kirchhoff plate theory requires C_1-continuity (ref. 17, p. 172); this leads to high order or nonconforming elements which is generally undesirable.

Another theory, that has been subject of most recent research in finite plate elements, is the Mindlin/Reissner theory (refs. 3 and 4). In the Mindlin theory, transverse shear deformation is included. Therefore Mindlin plate theory is applicable to modeling of classical thin plates as well as moderately thick, sandwich and composite plates (refs. 5 to 8). The basic assumption is that a straight line originally normal to the middle surface of the plate remains straight but not necessary normal to the middle surface during deformation. The vertical displacement is assumed not to vary through the plate thickness. Consequently, rotations are treated as independent variables. The finite element implementation requires only C_0-continuity (ref. 17, p. 172).

Despite its mathematical elegance, overstiff numerical results are obtained when using linear and quadratic elements for the analysis of thin plates. This problem is very common and often refers to as a "shear locking" phenomenon.

Several techniques have been proposed to remove the shear locking effect (refs. 9 and 10). However in the literature of finite strip, only two techniques are widely used. First, the use of "reduced integration" schemes for evaluation of the transverse shear components of the element stiffness matrix is applied by Mawenya and Davies (ref. 6) for three-node quadratic Mindlin strip element. Benson and Hinton (ref. 11) used the same technique but extended the analysis to vibration and stability problems. The second technique is the uses of polynomials of sufficiently high order to approximate the displacements. Onate and Suarez (ref. 12) used both techniques and compared the linear, quadratic, and cubic Mindlin strip elements using full, selective, and reduced integrations. Their conclusion is the two-node linear element with selective/reduced integration for the simplest and most efficient finite strip element. This agreed very well with the results of Hinton and Zienkiewicz (ref. 13).

A new, simple two-node linear finite strip plate bending element for the analysis of very thin to thick structures is presented here. The essential ingredient of this new element lies in an assumed strain distribution technique introduced by McNeal (ref. 14) and Dvorkin (ref. 15) for developing finite element plate and shell elements. A new transverse shear strain is proposed and then constrained to equal the conventional transverse shear strain at selected points.

In section 2, the standard Mindlin finite strip plate bending element formulation is presented. The new formulation is given in section 3. Particular attention is focussed on points of evaluation for transverse shear strain. In addition to the theoretical development, numerical results for different supports and loading conditions and a wide range of thickness are illustrated to assess the convergence and accuracy of the element are given in section 4.

NOMENCLATURE

A   cross sectional of plate

$\left[B_i^\ell\right]_b$ strain displacement matrix for bending at node i for the ℓth harmonic term

$\left[B_i^\ell\right]_s$ strain displacement matrix for shear at node i for the ℓth harmonic term

E   Young's Modulus

k   shear correction factor

N_i shape function for node i

q   transverse loading per unit area

$\{R_i^\ell\}$ externally applied load vector at node i for the ℓth harmonic term

2

r	natural coordinate variable
t	thickness of plate
$\{U_i^{\ell}\}$	nodal displacement vector at node i for the ℓth harmonic term
w	transverse displacement
w_i^{ℓ}	nodal displacement at node i for ℓ harmonic term
β_x	section rotation in x-direction
β_y	section rotation in y-direction
γ_{xz}, γ_{yz}	transverse shear strains
ε_b	bending strain
ε_s	transverse shear strain
$\theta_{x_i}^{\ell}$	nodal rotation in x-direction at node i for the ℓth harmonic term
$\theta_{y_i}^{\ell}$	nodal rotation in y-direction at node i for the ℓth harmonic term
κ	vector of curvature
σ_b	bending stress
σ_s	shear stress
ν	Poisson's ratio
π	total potential energy

2. FORMULATION OF MINDLIN/REISSNER STRIP ELEMENT

The finite strip method offers an alternative to the standard finite element method which uses polynomial functions in both x- and y-directions. The combination of polynomial and harmonic functions satisfy a priori the boundary conditions at the end of the strips and have the advantage of greatly reducing the number of equations to be solved for static analysis. For each type of supported condition at the strip ends, the necessary harmonic function is different. In this paper only simply supported conditions are considered.

Consider a typical finite strip plate element, whose mid-surface lies in the x-y plane, with thickness t, longitudinal width b, strip width a, as shown in figure 1. The z-axis is normal to the plate mid-surface and the plate is assumed to be loaded by a pressure q. The sign conventions for positive direction of the independent variables are illustrated in figure 1.

For a two-node linear strip element, both the transverse displacement w and the section rotations β_x and β_y within an element are interpolated in

3

terms of nodal displacements w_i^{ℓ} and nodal rotations $\theta_{x_i}^{\ell}$, $\theta_{y_i}^{\ell}$ as

$$w = \sum_{\ell=1}^{n} \sum_{i=1}^{2} N_i w_i^{\ell} S_{\ell}$$

$$\beta_x = \sum_{\ell=1}^{n} \sum_{i=1}^{2} N_i \theta_{y_i}^{\ell} S_{\ell} \qquad (1)$$

$$\beta_y = \sum_{\ell=1}^{n} \sum_{i=1}^{2} N_i \theta_{x_i}^{\ell} C_{\ell}$$

$$N_1 = \frac{1-r}{2}$$

$$N_2 = \frac{1+r}{2} \qquad (2)$$

r is the natural coordinate in x-direction

and

$$S_{\ell} = \sin\left(\frac{\ell \pi y}{b}\right); \quad C_{\ell} = \cos\left(\frac{\ell \pi y}{b}\right)$$

By using equation (1) simply supported boundary conditions are automatically satisfied at y = 0 and b,

$$w = \beta_x = \frac{\partial w}{\partial x} = \frac{\partial \beta_x}{\partial x} = \frac{\partial \beta_y}{\partial y} = 0 \qquad (3)$$

Bending and shear strains are introduced separately as follow:

<u>Bending Strains</u> (linear through the thickness)

$$\varepsilon_b = z_\kappa \qquad (4a)$$

where

$$\kappa = \begin{bmatrix} \beta_{x,x} \\ -\beta_{y,y} \\ \beta_{x,y} - \beta_{y,x} \end{bmatrix} = \sum_{\ell=1}^{n} \sum_{i=1}^{2} \left[B_i^{\ell} \right]_b \{ U_i^{\ell} \} \qquad (4b)$$

4

and $\left[B_i^{\ell}\right]_b$ is the strain-displacement matrix for bending at node i for the ℓth harmonic term which can be written as

$$\left[B_i^{\ell}\right]_b = \begin{bmatrix} 0 & 0 & \dfrac{\partial N_i}{\partial x} S_{\ell} \\[2ex] 0 & \dfrac{\ell \pi N_i S_{\ell}}{b} & 0 \\[2ex] 0 & -\dfrac{\partial N_i}{\partial x} C_{\ell} & \dfrac{\ell \pi N_i C_{\ell}}{b} \end{bmatrix} \tag{4c}$$

and $\{U_i^{\ell}\}$ is the nodal displacement vector as

$$\{U_i^{\ell}\} = \left\{ w_i^{\ell} \quad \Theta_{x_i}^{\ell} \quad \Theta_{y_i}^{\ell} \right\}^T$$

Transverse Shear Strains (constant through the thickness)

$$\varepsilon_s = \begin{bmatrix} \dfrac{\partial w}{\partial x} + \beta_x \\[2ex] \dfrac{\partial w}{\partial y} - \beta_y \end{bmatrix} = \sum_{\ell=1}^{n} \sum_{i=1}^{2} \left[B_i^{\ell}\right]_s \{U_i^{\ell}\} \tag{5a}$$

where $\left[B_i^{\ell}\right]_s$ is the strain-displacement matrix for shear at node i for the ℓth harmonic term which can be written as

$$\left[B_i^{\ell}\right]_s = \begin{bmatrix} \dfrac{\partial N_i}{\partial x} S_{\ell} & 0 & N_i S_{\ell} \\[2ex] \dfrac{\ell \pi N_i C_{\ell}}{b} & -N_i C_{\ell} & 0 \end{bmatrix} \tag{5b}$$

The state of stress in the plate corresponds to a plane stress assumption. Considering an isotropic linear elastic material, the stress-strain relations are:

$$\sigma_b = \begin{bmatrix} \sigma_x \\[1ex] \sigma_y \\[1ex] \tau_{xy} \end{bmatrix} = z \frac{E}{1-\nu^2} \begin{bmatrix} 1 & \nu & 0 \\[1ex] \nu & 1 & 0 \\[1ex] 0 & 0 & \dfrac{1-\nu}{2} \end{bmatrix} \kappa \tag{6}$$

5

and

$$\sigma_s = \begin{bmatrix} \tau_{xz} \\ \tau_{yz} \end{bmatrix} = \frac{E}{2(1 + \nu)} \, \varepsilon_s \tag{7}$$

where E is Young's modulus and ν is Poisson's ratio.

The total potential energy can be obtained as (ref. 17)

$$\pi = \frac{1}{2} \int_A \int_{-t/2}^{+t/2} \varepsilon_b^T \sigma_b \; dz dA + \frac{k}{2} \int_A \int_{-t/2}^{+t/2} \varepsilon_s^T \sigma_s \; dz dA - \int_A qw \; dA \tag{8}$$

where

t is the thickness of plate

A is the cross-sectional area of plate

q is transverse loading per unit area

k is shear correction factor to account for nonuniformity of the transverse shear stresses through the plate thickness (usually set equal to 5/6)

Substituting equation (1) and equations (4) to (7) into equation (8), the total potential energy can be rewritten as

$$\pi = \frac{1}{2} \int_A \kappa^T D_b \kappa \; dA + \frac{1}{2} \int_A \varepsilon_s^T D_s \varepsilon_s \; dA - \int_A \left(\sum_{\ell=1}^{n} \sum_{i=1}^{2} N_i w_i^\ell S_\ell \right) q dA \tag{9}$$

where

$$D_b = \frac{Et^3}{12\left(1 - \nu^2\right)} \begin{bmatrix} 1 & \nu & 0 \\ \nu & 1 & 0 \\ 0 & 0 & \frac{1 - \nu}{2} \end{bmatrix} \tag{10a}$$

$$D_s = \frac{Etk}{2(1 + \nu)} \begin{bmatrix} 1 & 0 \\ 0 & 1 \end{bmatrix} \tag{10b}$$

The loads are also resolved into a sine series in the y-direction similar to the displacement expression such that

6

$$q = \sum_{\ell=1}^{n} q_{\ell} S_{\ell} \tag{11a}$$

where for a distributed load per unit area from $y = c$ to $y = d$

$$q_{\ell} = \frac{2}{b} \int_{c}^{d} q(x,y) S_{\ell} dy \tag{11b}$$

The strip equilibrium equations are obtained by imposing the stationary condition on π, where w, β_x, and β_y are independent variables. Using the orthogonality properties of the harmonic series (ref. 8) as

$$\sum_{\ell=1}^{n} \sum_{i,j} \left[K_{ij}^{\ell} \right] \{ U_i^{\ell} \} = \sum_{\ell=1}^{n} \sum_{i} \{ R_i^{\ell} \} \tag{12}$$

where

$$\left[K_{ij}^{\ell} \right] = \int_{A} \left[B_i^{\ell} \right]_b^T \left[D_b \right] \left[B_j^{\ell} \right]_b dA + \int_{A} \left[B_i^{\ell} \right]_s^T \left[D_s \right] \left[B_j^{\ell} \right]_s dA \tag{13}$$

for a single strip with node i and j

$$\{ R_i^{\ell} \} = -\frac{b}{2} \int q_{\ell} \begin{bmatrix} N_1 & 0 & 0 & N_2 & 0 & 0 \end{bmatrix}^T dx \tag{14}$$

for node i under distributed load

or

$$\{ R_i^{\ell} \} = P \sin \left(\frac{\ell \pi c}{b} \right) \tag{15}$$

for node i under a concentrated load P at $y = c$

The total resulting stiffness matrix is

$$
\begin{bmatrix} [K^1] & & & & \\ & [K^2] & & & \\ & & \cdot & & \\ & & & \cdot & \\ & & & & [K^n] \end{bmatrix} \begin{bmatrix} U^1 \\ U^2 \\ \cdot \\ \cdot \\ \cdot \\ U^n \end{bmatrix} = \begin{bmatrix} R^1 \\ R^2 \\ \cdot \\ \cdot \\ \cdot \\ R^n \end{bmatrix}
\tag{16}
$$

where

$[K^\ell]$ is the global stiffness matrix for the ℓth harmonic term

$\{U^\ell\}$ is the global nodal displacement vector for the ℓth harmonic term

and

$\{R^\ell\}$ is the global externally applied load vector for the ℓth harmonic term

Equation (12) reflects the uncoupling of the stiffness matrix that leads to independent sets of equilibrium equations for each harmonic term. This fact can be taken advantage in simply supported case. That is, for other boundary conditions, the different harmonic terms may not always uncouple and a full stiffness matrix may have to be evaluated.

3. ASSUMED STRAIN DISTRIBUTIONS

The finite strip formulation presented in the previous section has some drawback. The element locks when the thickness is very thin using two-point Gauss quadrature integration for both bending and shear stiffness. This is due to the fact that the shear stiffness terms are overwhelming the bending stiffness terms and this leads to an overstiff element even though a very fine mesh is used. In the past this excessive stiffness may be attributed to "spurious shear" effects which were suppressed by reducing the order of the integration rule (ref. 9). To circumvent this locking phenomenon even though selective and reduced integration is a well-established approach, an assumed strain distribution technique (refs. 14 and 15) is employed here.

For each strip element, instead of using equation (5), new transverse shear strains are introduced as

$$
\gamma_{xz}^\ell = \frac{1}{2} \left(\gamma_{xz}^A + \gamma_{xz}^C \right)
$$

$$
\gamma_{yz}^\ell = \frac{1}{2} \left(\gamma_{yz}^B + \gamma_{yz}^D \right)
\tag{17}
$$

where γ_{xz}^A and γ_{xz}^C are the transverse shear strains evaluated at points A

8

and C with r = 0, y = b/4, and y = 3b/4 respectively (see fig. 2) using equation (5) as

$$\gamma_{xz}^{A} = \frac{1}{2} \, S_{\ell}^{A} \left[\frac{-w_1^{\ell}}{J} + \theta_{y_1}^{\ell} + \frac{w_2^{\ell}}{J} + \theta_{y_2}^{\ell} \right]$$

$$\gamma_{xz}^{C} = \frac{1}{2} \, S_{\ell}^{C} \left[\frac{-w_1^{\ell}}{J} + \theta_{y_1}^{\ell} + \frac{w_2^{\ell}}{J} + \theta_{y_2}^{\ell} \right]$$

(18)

with $S_{\ell}^{A} = \sin(3\ell\pi/4)$, $S_{\ell}^{C} = \sin(\ell\pi/4)$, and $J = a/2$, and γ_{yz}^{B}, γ_{yz}^{D} are also the transverse shear strains evaluated at points B and C with r at Gauss points and y = b/4, respectively (see fig. 2) using equation (5) as

$$\gamma_{yz}^{B} = C_{\ell}^{B} \left[\frac{1 + \sqrt{3}}{2} \left(\frac{\ell\pi}{b}\right) w_1^{\ell} - \frac{1 + \sqrt{3}}{2} \theta_{x_1}^{\ell} + \frac{1 - \sqrt{3}}{2} \left(\frac{\ell\pi}{b}\right) w_2^{\ell} - \frac{1 - \sqrt{3}}{2} \theta_{x_2}^{\ell} \right]$$

(19)

$$\gamma_{yz}^{D} = C_{\ell}^{D} \left[\frac{1 - \sqrt{3}}{2} \left(\frac{\ell\pi}{b}\right) w_1^{\ell} - \frac{1 - \sqrt{3}}{2} \theta_{x_1}^{\ell} + \frac{1 + \sqrt{3}}{2} \left(\frac{\ell\pi}{b}\right) w_2^{\ell} - \frac{1 + \sqrt{3}}{2} \theta_{x_2}^{\ell} \right]$$

with $C_{\ell}^{B} = C_{\ell}^{D} = \cos(\ell\pi/4)$.

Hence, equation (17) can be rewritten with the new shear-strain displacement matrix as

$$\varepsilon_s = \sum_{\ell=1}^{n} \begin{bmatrix} \gamma_{xz}^{\ell} \\ \\ \gamma_{yz}^{\ell} \end{bmatrix} = \sum_{\ell=1}^{n} \left[B^{\ell} \right]_s \{ U_{e1}^{\ell} \}$$

(20a)

where

$$\left[B^{\ell} \right]_s = \begin{bmatrix} -\dfrac{\left(S_{\ell}^{A} + S_{\ell}^{C} \right)}{4J} & 0 & \dfrac{\left(S_{\ell}^{A} + S_{\ell}^{C} \right)}{4} & \dfrac{\left(S_{\ell}^{A} + S_{\ell}^{C} \right)}{4J} & 0 & \dfrac{\left(S_{\ell}^{A} + S_{\ell}^{C} \right)}{4J} \\ \\ \left(\dfrac{\ell\pi}{b}\right) C_{\ell}^{B} & \dfrac{-C_{\ell}^{B}}{2} & 0 & \left(\dfrac{\ell\pi}{b}\right) C_{\ell}^{D} & \dfrac{-C_{\ell}^{D}}{2} & 0 \end{bmatrix}$$

(20b)

and

$$\{ U_{e1}^{\ell} \} = \left\{ w_1^{\ell} \quad \theta_{x_1}^{\ell} \quad \theta_{y_1}^{\ell} \quad w_2^{\ell} \quad \theta_{x_2}^{\ell} \quad \theta_{y_2}^{\ell} \right\}^{T}$$

(20c)

9

Notice that the assumed shear strains are constant throughout the cross-sections and constrained to equal the shear strains of equation (5) at selected points. The choice of these points is of paramount importance in evaluating the predictive capability of the element even though the assumed strain distributions in equation (17) are the integral part of the overall performance. With the shear strain displacement matrix of equation (20b) replacing equation (5b) the element stiffness matrix is formed explicitly as shown in figure 3 using exact order of integration.

4. EVALUATION OF THE NEW FINITE STRIP ELEMENT

The new finite strip element has been implemented into the finite element computer program FEAP (ref. 18) with relative ease. The subroutines written in FORTRAN 77 for the formulation of the element stiffness matrix consists of approximately 200 lines. All the results presented in this paper were obtained using double precision arithmetic on an IBM/PC-AT.

Numerical problems have been tested in this section to show the performance of the new element. The results are presented for different aspects: mesh size and harmonic term convergence characteristics, shear locking phenomenon as the thickness decreases, and shear force and bending moment prediction. Exact order of numerical integration is employed. Spurious zero energy mode effect (ref. 17) were not observed for the problems tested and the boundary conditions specified. Some of these results are compared with the analytical results obtained by other investigators (refs. 19 and 20).

Shear Locking Investigation

Using eight strip elements with four nonzero harmonic terms and $\nu = 0.3$, a simply supported square plate under two loading conditions: uniform and concentrated loads, is investigated with a wide range of span/thickness ratio from 5 to 10^5. The deflection at the center and quarter of the plate are plotted for both the full and reduced integrations of the troublesome transverse shear strain element, in figure 4 (uniform load case) and in figure 5 (concentrated load case). Shear locking was not detected for the entire range of aspect ratios for the new element and reduced integration element. If the element was to exhibit shear locking as seen in the case of full integration of troublesome transverse shear strain, the displacements would be significantly less and less as the thickness decreased, due to overly stiff element behavior. Note that for the uniform load case the even harmonic terms are always zero as well as for the central concentrated load case. If however, the concentrated load was not located at the center, all the harmonic terms must be included.

Convergence of Mesh Size and Harmonic Term

To assess the convergence characteristics of the new element, a simply supported, uniformly loaded, square plate with t/b ratio equal to 0.01 and $\nu = 0.3$ is considered. For mesh convergence, the central deflections, central bending moments in both the x- and y-directions are tabulated in table I for four different meshes as well as the exact solution (ref. 19). Bending moments shown are linearly extrapolated from the Gauss points to the node. Also in the table, the number of degrees of freedom for each mesh is shown. This gives a

more realistic view of the computational cost. Graphical representation is shown in figure 6 by plotting percentage of error of the central deflections and central bending moment in the x-direction with mesh size. Good solutions are reached with only four strips and single harmonic term for both displacement and moment. The central deflection and bending moment for a four-node plate finite element (ref. 15) are also plotted in figure 6 for comparison purposes. This shows how rapid the rate of convergence is with no sign of shear locking.

For the convergence of harmonic term, eight strip element mesh is used and the numerical results are tabulated in table II with four nonzero harmonic terms. Fairly good convergence is again obtained. Errors are less than 0.4 percent when the third nonzero harmonic term is specified for both quantities (see fig. 7). However the number of nonzero harmonic terms required for the analysis of more complicated problems may be increased. Note that this element is a low-order two-node strip. Numerical computation is minimum but convergence rate is relatively high.

Predictions of Shear Force and Bending Moment

For low-order element the standard finite strip formulation based on Mindlin/Reissner plate theory is well recognized to predict accurate displacements and fairly good bending moments when the selective and reduced integration technique or high-order element is used (ref. 12). However, the shear force predictions are poor (see figs. 8 to 12) and hardly found in the finite strip literature even though they can be important in designing structures such as bridges and slabs. Therefore, the shear force predictive capability of this new finite strip element is studied and presented here. Due to the limited availability of analytical solutions, only four cases for shear forces and one case for bending moment are compared.

The uniformly loaded square plates involving a variety of support conditions in the x-direction are investigated. In order to capture the steep gradient of the dependent variables near a plate edge, a rather fine mesh is modeled in the analysis with the new strip element. The results for variations of shear forces and bending moments across the mid-plate in the various cases are plotted with analytical solutions by Kant and Hinton (ref. 20) in figures 8 to 12. These analytical solutions based on Mindlin plate theory assume the transverse displacement and sectional rotations similar to standard finite strip element. The system of differential equations is used and then numerically integrated using the so-called "segmentation method." The authors in that paper claimed that the analytical results compared favorably well with the finite strip method.

The results of shear force and bending moment shown in figures 8 to 12 along with the pertinent data and boundary conditions are in good agreement near the center of the plates. In the regions away from the center, the differences start to magnify and are approximately average at 15 percent near the edge of mid-plate. However, the curves for both solutions seem to follow the same pattern. Note that our element is only a simple, two-node linear element and its predictive capabilities (see figs. 8 to 12) are shown to exceed previously developed elements.

5. CONCLUDING REMARKS

A two-node linear finite strip element based on Mindlin/Reissner plate theory is presented for static analysis of plates. A new shear strain distribution is assumed and connected to the standard shear strains at selected points. These points are chosen to remove shear locking phenomenon without the need for "reduced integration" technique. Due to the uncoupling nature of the finite strip method, the element stiffness matrix can be explicitly formulated for efficient computation and computer implementation.

Several numerical studies were performed to assess the numerical performance of the aforementioned finite strip element. Based on the results obtained, the following characteristics of the element can be stated:

1. Simple, reliable, and efficient in computations

2. Good convergence characteristics both in mesh size and harmonic term

3. No shear locking effect for very thin situations

4. Fairly accurate moment and shear force predictions

5. Applicable to both thin and thick structures

REFERENCES

1. Cheung, Y.K.: The Finite Strip Method in the Analysis of Elastic Plates with Two Opposite Simply Supported Ends. Proc. Inst. Civ. Eng., vol. 40, May 1968, pp. 1-7.

2. Cheung, Y.K.: Finite Strip Method of Analysis of Elastic Slabs. Proc. Am. Soc. Civ. Eng. J. Eng. Mech. Div., vol. 94, no. EM6, Dec. 1968, pp. 1365-1378.

3. Mindlin, R.D.: Influence of Rotatory Inertia and Shear on Flexural Motions of Isotropic Elastic Plates. J. Appl. Mech., vol. 18, no. 1, Mar. 1951, pp. 31-38.

4. Reissner, E.: The Effect of Transverse Shear Deformation on the Bending of Elastic Plates. J. Appl. Mech., vol. 12, no. 2, June 1945, pp. 69-77.

5. Mawenya, A.S.: Finite Element Analysis of Sandwich Plate Structures. Ph.D. Thesis, University of Wales, 1973.

6. Mawenya, A.S.; and Davies, J.D.: Finite Strip Analysis of Plate Bending Including Transverse Shear Effects. Build. Sci., vol. 9, no. 3, Sept. 1974, pp. 175-180.

7. Azizian, Z.G.; and Dawe, D.J.: Analysis of the Large Deflection Behaviour of Laminated Composite Plates Using the Finite Strip Method. Composite Structures 3, I.H. Marshall, ed., Elsevier Applied Science, London, 1985, pp. 677-691.

8. Cheung, Y.K.: The Finite Strip Method in Structural Analysis, Pergamon Press, 1976.

9. Hughes, T.J.R.; Cohen, M.; and Haroun, M.: Reduced and Selective Integration Techniques in the Finite Element Analysis of Plates. Nucl. Eng. Des., vol. 46, no. 1, Mar. 1978, pp. 203-222.

10. Zienkiewicz, O.C.; Taylor, R.L.; and Too, J.M.: Reduced Integration Technique in General Analysis of Plates and Shells. Int. J. Numer. Meth. Eng., vol. 3, no. 2, Apr.-June 1971, pp. 275-290.

11. Benson, P.R.; and Hinton, E.: A Thick Finite Strip Solution for Static, Free Vibration and Stability Problems. Int. J. Numer. Meth. Eng., vol. 10, no. 3, 1976, pp. 665-678.

12. Onate, E.; and Suarez, B.: A Comparison of the Linear, Quadratic and Cubic Mindlin Strip Elements for the Analysis of Thick and Thin Plates. Comput. Struct., vol. 17, no. 3, 1983, pp. 427-439.

13. Hinton, E.; and Zienkiewicz, O.C.: A Note on a Simple Thick Finite Strip. Int. J. Numer. Meth. Eng., vol. 11, no. 5, 1977, pp. 905-907.

14. MacNeal, R.H.: Derivation of Element Stiffness Matrices by Assumed Strain Distributions, Nucl. Eng. Des., vol. 70, no. 1, June (I) 1982, pp. 3-12.

15. Dvorkin, E.N.; and Bathe, K.J.: A Continuum Mechanics Based Four-Node Shell Element for General Nonlinear Analysis. Eng. Comput., vol. 1, 1984, pp. 77-88.

16. Onate, E.; and Suarez, B.: A Unified Approach for the Analysis of Bridges, Plates and Axisymmetric Shells Using the Linear Mindlin Strip Element. Comput. Struct., vol. 17, no. 3, 1983, pp. 407-426.

17. Bathe, K.J.: Finite Element Procedure in Engineering Analysis. Prentice-Hall, 1982.

18. Zienkiewicz, O.C.: The Finite Element Method. 3rd ed., McGraw Hill, 1982.

19. Timoshenko, S.; and Woinowsky-Krieger, S.: Theory of Plates and Shells. 2nd ed., McGraw-Hill, New York, 1959.

20. Kant, T., and Hinton, E.: Mindlin Plate Analysis by Segmentation Method. J. Eng. Mech., vol. 109, no. 2, Apr. 1983, pp. 537-556.

TABLE I. - CONVERGENCE STUDY OF MESH SIZE FOR A SIMPLY
SUPPORTED SQUARE PLATE UNDER UNIFORM LOAD
WITH FOUR NONZERO HARMONIC TERMS
[b/t = 100 and ν = 0.3.]

No. of DOF	No. of strips	Central displacement, W(qb/D)	Central bending moments[a]	
			Mx(qb)	My(qb)
5	2	0.00348	0.03691	0.03865
11	4	.00401	.04785	.04699
17	6	.00404	.04799	.04753
23	8	.00405	.04794	.04766
Exact		0.00406	0.0479	0.0479

[a]Linearly extrapolated from the Gauss points.

TABLE II. - CONVERGENCE STUDY OF HARMONIC TERMS FOR A
SIMPLY SUPPORTED SQUARE PLATE UNDER UNIFORM LOAD
[b/t = 100 and ν = 0.3.]

Harmonic term	Central displacement, W(qb/D)	Central bending moments[a]	
		Mx(qb)	My(qb)
$\ell = 1$	-0.004101	-0.04930	-0.05162
$\ell = 3$	.000051	.00158	.00461
$\ell = 5$	-.000004	-.00032	-.00103
$\ell = 7$	.000001	.00011	.00038
Sum	-.004054	-.04794	-.04766
Exact	-0.00406	-0.0479	-0.0479

[a]Linearly extrapolated from the Gauss points.

14
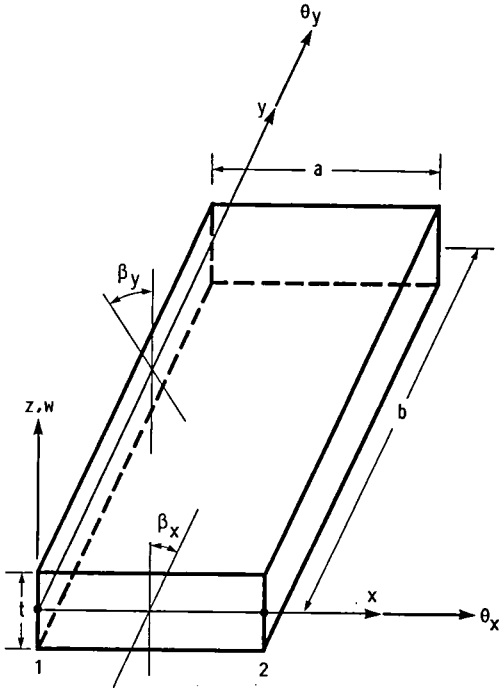
FIGURE 1. – VIEW OF SINGLE STRIP ELEMENT AND NOTATIONS USED.
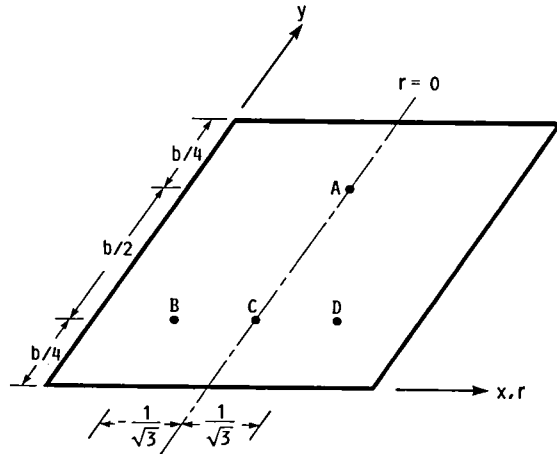
FIGURE 2. – SELECTED POINTS FOR ASSUMED SHEAR STRAINS IN EACH ELEMENT. ONE STRIP ELEMENT WITH $x = a$, AND $y = b$.

$$[K]^{\ell} = \begin{bmatrix}
D_4\left(\dfrac{4bH^2}{a} + \dfrac{abF^2}{4}c\right) & -D_4\dfrac{ab}{4}\cdot FC & -2bH^2D_4 & -D_4\left(\dfrac{4bH^2}{a} + \dfrac{abF^2}{4}c\right) & -D_4\dfrac{ab}{4}\cdot FC & -2bH^2D_4 \\[2ex]
 & \dfrac{b}{2}\left(D_1F^2\dfrac{a}{3} + \dfrac{D_3}{a} + D_4\dfrac{a}{2}c\right) & \dfrac{bF}{4}(D_3 - D_2) & -D_4\dfrac{ab}{4}\cdot FC & \dfrac{b}{2}\left(D_1F^2\dfrac{a}{6} - \dfrac{D_3}{a} + D_4\dfrac{a}{2}c\right) & \dfrac{bF}{4}(D_2 + D_3) \\[2ex]
 & & b\left(\dfrac{D_1}{2a} + D_3F^2\dfrac{a}{6} + D_4aH^2\right) & 2D_4bH^2 & -\dfrac{bF}{4}(D_2 + D_3) & b\left(-\dfrac{D_1}{2a} + D_3F^2\dfrac{a}{12} + D_4aH^2\right) \\[2ex]
 & & & D_4\left(\dfrac{4bH^2}{a} + \dfrac{abF^2}{4}c\right) & -D_4\dfrac{ab}{4}\cdot FC & 2bH^2D_4 \\[2ex]
 & \text{SYMMETRIC} & & & \dfrac{b}{2}\left(D_1F^2\dfrac{a}{3} + \dfrac{D_3}{a} + D_4\dfrac{a}{2}c\right) & \dfrac{bF}{4}(D_2 - D_3) \\[2ex]
 & & & & & b\left(\dfrac{D_1}{2a} + D_3F^2\dfrac{a}{6} + D_4aH^2\right)
\end{bmatrix}$$

$$D_1 = \frac{Et^3}{12(1-\nu^2)} \qquad D_2 = \frac{Et^3\nu}{12(1-\nu^2)} \qquad C = \cos^2\left(\frac{\ell\pi}{4}\right) \qquad F = \frac{\ell\pi}{b} \qquad D_3 = \frac{Et^3}{24(1+\nu)} \qquad D_4 = \frac{Etk}{2(1+\nu)} \qquad H = 0.25\left(\sin 3\frac{\ell\pi}{4} + \sin\frac{\ell\pi}{4}\right)$$

E = YOUNG'S MODULUS $\qquad \nu$ = POISSON'S RATIO

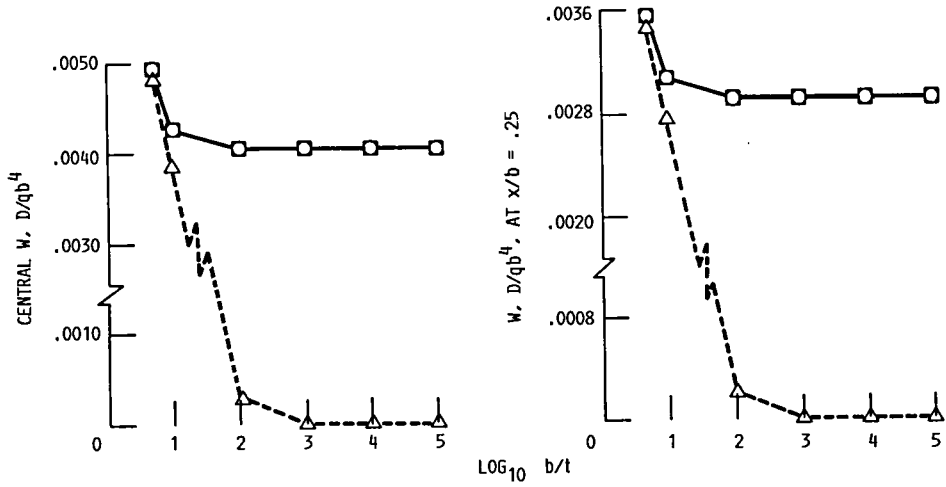FIGURE 3. – ELEMENT STIFFNESS OF NEW STRIP ELEMENT FOR 1TH NONZERO HARMONIC TERM.

FIGURE 4. - SPAN/THICKNESS RATIO STUDY OF SIMPLY SUPPORTED SQUARE PLATE UNDER UNIFORM LOAD WITH FOUR NONZERO HARMONIC TERMS.
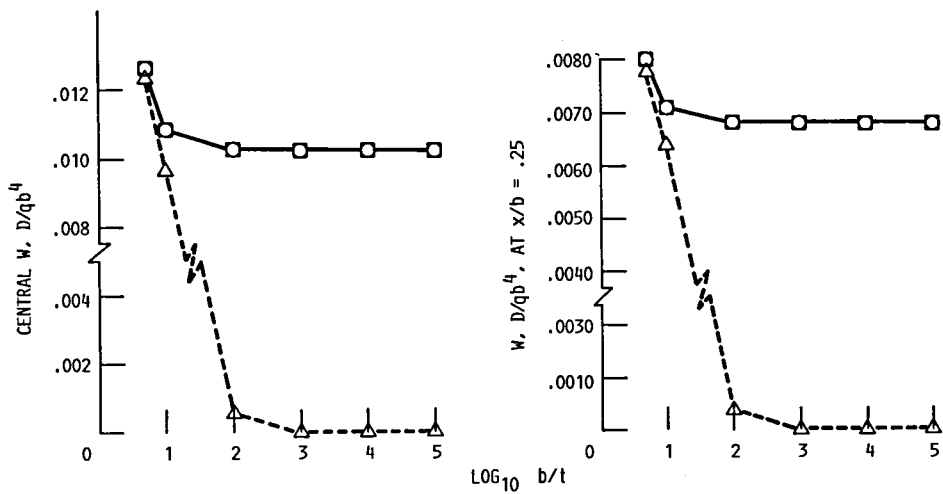

FIGURE 5. - SPAN/THICKNESS RATIO STUDY OF SIMPLY SUPPORTED SQUARE PLATE UNDER CONCENTRATED LOAD WITH FOUR NONZERO HARMONIC TERMS.
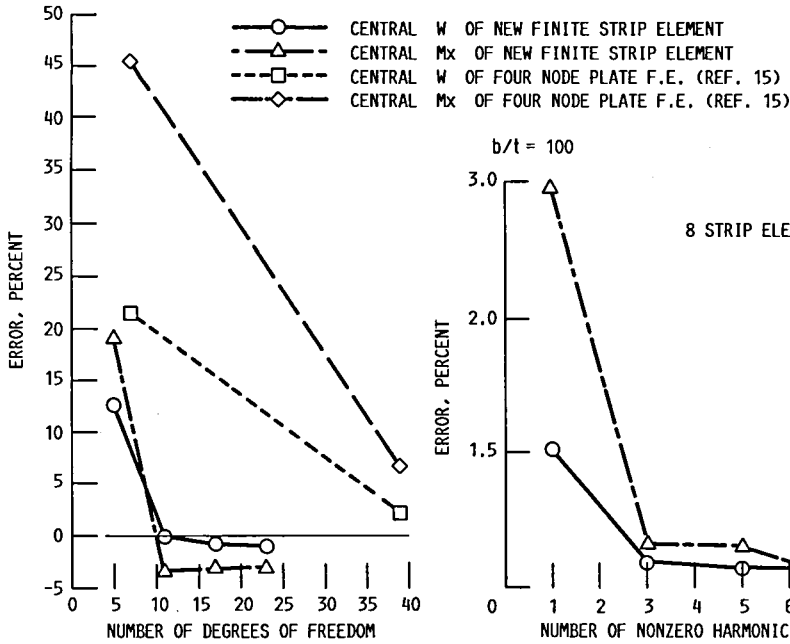
16

FIGURE 6. - MESH CONVERGENCE STUDY FOR
SIMPLY SUPPORT SQUARE PLATE UNDER
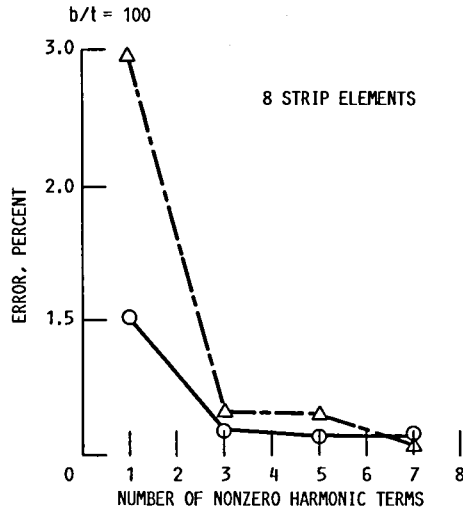UNIFORM LOAD (ν = 0.3) WITH ONE HAR-
MONIC TERM.

FIGURE 7. - CONVERGENCE STUDY WITH NUMBER
OF NONZERO HARMONIC TERMS FOR SIMPLY
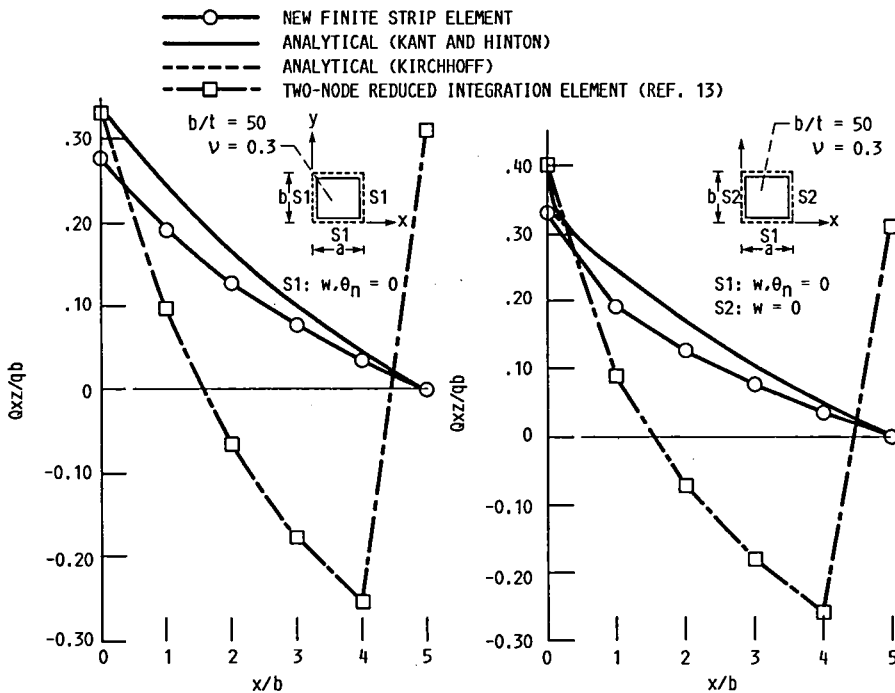SUPPORT SQUARE PLATE UNDER UNIFORM LOAD
(ν = 0.3).

FIGURE 8. - VARIATION OF SHEAR FORCE
Q_{xz} ALONG Y/b = 0.5 FOR SQUARE
PLATE UNDER UNIFORM LOAD WITH FOUR
NONZERO HARMONIC TERMS.

FIGURE 9. - VARIATION OF SHEAR FORCE
Q_{xz} ALONG Y/b = 0.5 FOR SQUARE
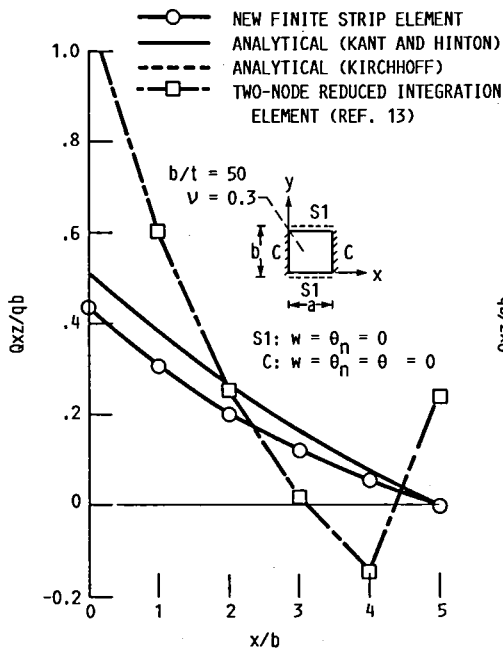PLATE UNDER UNIFORM LOAD WITH FOUR
NONZERO HARMONIC TERMS.

17

NEW FINITE STRIP ELEMENT
ANALYTICAL (KANT AND HINTON)
ANALYTICAL (KIRCHHOFF)
TWO-NODE REDUCED INTEGRATION
ELEMENT (REF. 13)

FIGURE 10. - VARIATION OF SHEAR FORCE
Qxz ALONG y/b = 0.5 FOR SQUARE
PLATE UNDER UNIFORM LOAD WITH FOUR
NONZERO HARMONIC TERMS.

FIGURE 11. - VARIATION OF SHEAR FORCE
Qxz ALONG y/b = 0.5 FOR SQUARE
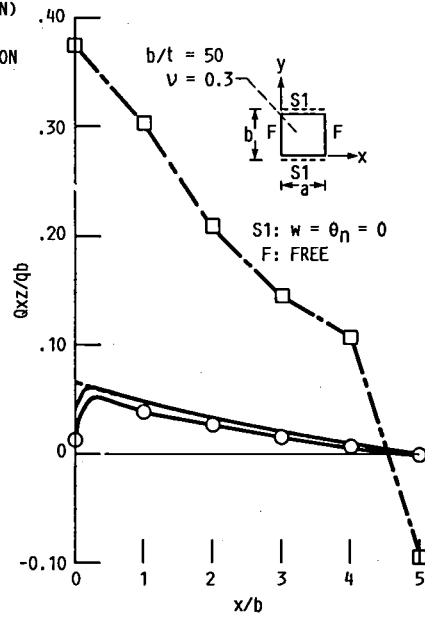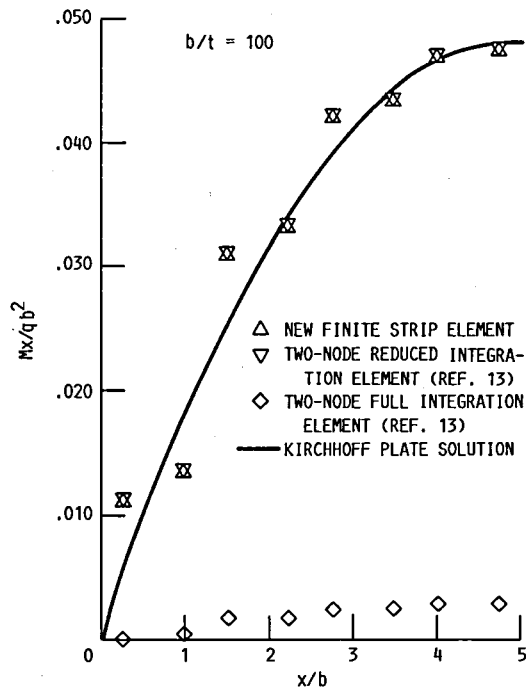PLATE UNDER UNIFORM LOAD WITH FOUR
NONZERO HARMONIC TERMS.

△ NEW FINITE STRIP ELEMENT
▽ TWO-NODE REDUCED INTEGRA-
TION ELEMENT (REF. 13)
◇ TWO-NODE FULL INTEGRATION
ELEMENT (REF. 13)
—— KIRCHHOFF PLATE SOLUTION

FIGURE 12. - VARIATION OF MOMENT Mx ALONG
y/b = 0.5 FOR SIMPLY SUPPORTED SQUARE PLATE
UNDER UNIFORM LOAD WITH FOUR NONZERO HAR-
MONIC TERMS (ν = 0.3).

18

Report Documentation Page

1. Report No. NASA TM-100928 ICOMP-88-12	2. Government Accession No.	3. Recipient's Catalog No.
4. Title and Subtitle Improved Finite Strip Mindlin Plate Bending Element Using Assumed Shear Strain Distributions		5. Report Date July 1988
		6. Performing Organization Code
7. Author(s) Abhisak Chulya and Robert L. Thompson		8. Performing Organization Report No. E-4194
		10. Work Unit No. 535-07-01
9. Performing Organization Name and Address National Aeronautics and Space Administration Lewis Research Center Cleveland, Ohio 44135-3191		11. Contract or Grant No.
12. Sponsoring Agency Name and Address National Aeronautics and Space Administration Washington, D.C. 20546-0001		13. Type of Report and Period Covered Technical Memorandum
		14. Sponsoring Agency Code

15. Supplementary Notes

16. Abstract

A linear finite strip plate element based on Mindlin/Reissner plate theory is developed. The analysis is suitable for both thin and thick plates. In the formulation new transverse shear strains are introduced and assumed constant in each two-node linear strip. The element stiffness matrix is explicitly formulated for efficient computation and computer implementation. Numerical results showing the efficiency and predictive capability of the element for the analysis of plates are presented for different support and loading conditions and a wide range of thicknesses. No sign of shear locking phenomenon was observed with the newly developed element.

17. Key Words (Suggested by Author(s)) Finite strip; Assumed strain distribution; Mindlin/Reissner plate theory; Shear locking; Explicitly formulated stiffness matrix	18. Distribution Statement Unclassified - Unlimited Subject Category 39		
19. Security Classif. (of this report) Unclassified	20. Security Classif. (of this page) Unclassified	21. No of pages 20	22. Price* A02

National Aeronautics and
Space Administration

Lewis Research Center
ICOMP (M.S. 5-3)
Cleveland, Ohio 44135

Official Business
Penalty for Private Use $300

FOURTH CLASS MAIL

ADDRESS CORRECTION REQUESTED

NASA